Factors Affecting Interdiffusion Rates in Films Prepared from Latex Particles with a Surface Rich in Acid Groups and Their Salts[1]

Haeng-Boo Kim[2] and Mitchell A. Winnik*

Department of Chemistry and Erindale College, University of Toronto, 80 St. George Street, Toronto, Canada M5S 1A1

Received June 22, 1994; Revised Manuscript Received January 4, 1995®

ABSTRACT: We report measurements of the kinetics of polymer diffusion in latex films prepared from pairs of poly(butyl methacrylate) [PBMA] latex particles. One set contains only a small amount of sulfate groups; the others contain significant amounts of carboxylic acid groups at the surface. Neutralization of these acid groups with sodium and barium hydroxide retards the interdiffusion rate but does not suppress it. In these experiments, we employ pairs of particles identical in size, with very similar molecular weights, molecular weight distributions, and surface charge densities, that differ only in the fluorescent chromophore (phenanthrene [Phe] or anthracene [An]) used to label the polymer. Each pair of latexes allows us to use direct nonradiative transfer [DET] experiments to follow polymer interdiffusion in films prepared from their dispersions. Acid group neutralization in the latex converts an acid-rich phase at the interparticle boundary in the film into an ionomer phase. Ba^{2+} salts are more effective than Na^+ at slowing down the polymer diffusion rate, and their influence increases in proportion to the amount of polar groups present. We follow an approach developed by Eisenberg (*Macromolecules* **1971**, *4*, 125) to estimate the T_g values of the ionomer phase in each film and show that there is a linear relationship between the mean apparent diffusion coefficient of the polymer determined from the DET experiment and $T - T_g$, where T is the annealing temperature of the film.

Introduction

Films prepared from aqueous dispersions of latex particles are widely used as coatings.[3] When freshly applied, the films formed are mechanically weak, but their strength grows upon aging or annealing.[4] In simple homopolymer films, this growth in strength can be correlated with the diffusion of polymer molecules across the interparticle boundary.[5,6] Theory suggests,[3] and experiments support the idea, that full strength of the joint is achieved when the polymer molecules near the latex surface have diffused across the interface a distance comparable to their root-mean squared radius of gyration.[7–11]

This paper addresses the issue of polymer interdiffusion in films prepared from latex particles in which the latex microspheres have a significant concentration of acid groups at their surface. These films are significantly more complex, in terms of both their composition and their morphology than simple homopolymer latex films. If the local density of the polar groups is sufficiently high, the polymer at the surface of the latex will form a separate interconnected phase in the newly formed film. This membrane separating the cells of the core polymer could act as a barrier to prevent or retard polymer diffusion between cells in these films. Furthermore, it is possible that in these films, the mechanical properties might arise through interaction between the polar surface groups rather than from polymer interdiffusion. Since so many aspects of the coatings industry rely on latex with a shell rich in acid groups, it is important, not only from a scientific point of view but also from a technological perspective, to understand interdiffusion in these latex films.

Latex particles containing a small number of sulfuric acid groups are produced by emulsion polymerization in which persulfate is used as a water soluble initiator. A more common practice is to add acrylic acid or methacrylic acid as part of the monomer feed. This introduces surface carboxylic acid groups on the latex which enhance its colloidal stability. It is widely believed in the coatings industry that the presence of these acid groups not only provides colloidal stability in the latex dispersion, but, for certain applications, also enhances the properties of the films formed. Two of the variables that enter into product development in the coatings industry are control over the amount of acid comonomer added to an emulsion polymerization reaction and the timing of its addition to the reaction.

While there are a variety of strategies for introducing acid groups into a latex particle, there are two relatively well-defined limiting approaches. First, one can begin by copolymerizing acrylic acid [AA] with a more hydrophobic monomer (e.g. styrene [S] or butyl acrylate [BA]) to produce a hydrophobically modified PAA. This copolymer will serve as a steric stabilizer in the subsequent polymerization of the hydrophobic monomer, yielding latex with a shell composed of slightly modified PAA.[12] Alternatively, one could prepare a seed latex using traditional initiators and surfactant and then add the acid comonomer in a subsequent polymerization stage. The feed for this final stage might typically be composed of 6–10 mol % methacrylic acid [MAA], so that the latex as a whole would contain 2–4 wt % acid comonomer. In these latexes, one presumes that the acid groups are present as part of a copolymer located primarily in the outer shell of the particle.

We have reported the synthesis and characterization of a latex system corresponding to the second type described above.[13] We prepared a series of poly(butyl methacrylate) [PBMA] latex particles by a three-stage emulsion polymerization process in which MAA was introduced in the final stage. For each sample, two pairs of latexes were prepared, one labeled with phenanthrene groups and the other, with anthracene. These serve as donor [D-] and acceptor [A-] groups, respec-

® Abstract published in *Advance ACS Abstracts,* February 15, 1995.

0024-9297/95/2228-2033$09.00/0

Table 1. Characteristics of PBMA and P(BMA-*co*-MAA) Latex Particles

	particle size (nm)	$10^5 M_w$ (M_w/M_n)	charge density (μequiv/g)			parking area (Å²/acid)
			$Q_s(SO_4H)^a$	$Q_s(CO_2H)^a$	$Q_b{}^b$	
An-MA0	129	4.8 (3.6)	10	0	35	730
Phe-MA0	127	4.1 (3.2)	9.9	0	32	750
An-MA2	152	4.8 (2.9)	5.2	40	84	140
Phe-MA2	147	4.4 (3.2)	5.8	44	88	130
An-MA4	150	4.2 (2.9)	4.8	75	122	79
Phe-MA4	150	4.0 (2.7)	4.4	61	117	96
An-MA6	149	4.9 (3.0)	4.2	112	260	55
Phe-MA6	146	4.3 (2.6)	4.8	116	270	54

[a] $Q_s(SO_4H)$ and $Q_s(COOH)$ are the moles of titratable acid groups per gram solids of latex. [b] Q_b is the total acid content of the latex in moles of acid groups per gram solids.

tively, for fluorescent nonradiative energy transfer studies of polymer interdiffusion in their films. In order to ensure that both the D- and A- labeled latex had common diameters and very similar molecular weights and molecular weight distributions, both samples were prepared from a common (unlabeled) seed latex.

In the second stage, BMA was polymerized using potassium persulfate as the initiator to yield a pair of latex samples containing a low density of $-OSO_3^-$ groups at the surface. This sample, MA0, was then used as the seed latex in the third-stage polymerization in which a mixture of BMA and MA were fed into the reaction under monomer-starved conditions. Three pairs of samples were prepared in this way, MA2, MA4, and MA6, containing increasing amounts of acid groups in the shell. The acid group content of each latex, following ion exchange, was determined by careful potentiometric titration in water and compared to the acid group content determined by dissolution of the latex polymer in tetrahydrofuran, followed by titration with sodium methoxide in methanol. The characteristics of these latexes are summarized in Table 1 and Figure 1.

In energy transfer experiments on films prepared from these dispersions, we observed interdiffusion by energy transfer to occur at the earliest stages of the annealing process.[13] Interdiffusion was retarded by the presence of the acid groups, but not suppressed. Neutralization of the acid groups with sodium or barium hydroxide led to further retardation of the interdiffusion process.[14] The barium salt was much more effective than the sodium salt in slowing down polymer interdiffusion, and the two salts were in turn much more effective than the unneutralized −COOH groups. In addition, we observed that the extent of diffusion inhibition increased with the extent of acid group neutralization. To us this suggests that in the films formed from these microspheres, an ionomer membrane phase forms. In these experiments, both the core and comonomer phase of the latex were similarly labeled with donor and acceptor dyes. For energy transfer to be observed, either the polymers in the ionomer phase must interdiffuse or the core polymer must diffuse through this membrane. The details of this mixing process are far from clear.

Here we examine these systems in more detail, using temperature and extent of acid group neutralization as variables. On the basis of these sum of these results, we propose a model, developed in terms of the glass transition temperature T_g of the polar shell polymer, to explain our observations.

Experimental Section

The latex samples MA0, MA2, MA4, and MA6 are the same samples whose syntheses and characterization have been previously reported.[13] Each latex disperion in water, following ion exchange, was titrated with KOH and then back-titrated with HCl solutions to determine the number of titratable acid groups per gram of solids, Q_s. Dried samples of the same latex were dissolved in tetrahydrofuran and titrated with sodium methoxide in methanol to determine the total acid content, Q_T. Relevant details are given in Table 1. Films were prepared from a dispersion containing an equal number of Phe- and An-labeled particles. To this mixture (0.30 g) was added a known amount of base, either sodium or barium hydroxide, and the sample was allowed to stand for ca. 30 min at room temperature. Except in one experiment, the amount of base was chosen to be equal to the amount of titratable acid groups. A few drops of the dipersion were placed on a small quartz plate (ca. 5 mm × 10 mm) previously warmed on a hot plate to 32 °C. A Petri dish was inverted over the film to slow down the drying process. Drying occurred over a period of ca. 4 h to yield transparent and void-free films 30−50 μm thick. To anneal films for short periods of time, the quartz substrates supporting the films were placed directly on a high-mass aluminum slab inside a convection over prewarmed to the appropriate temperature (±1 °C). For films annealed for longer periods of time, steps were taken to prevent polymer and chromophore oxidation. The films were placed inside small test tubes which were sealed with septa. Using flowing gas and syringe needles, an argon atmosphere was introduced into the test tube, and the test tube was placed into the oven. Samples were removed from the oven and cooled to room temperature for fluorescence measurements.

Samples for fluorescence decay measurements were placed in a small quartz test tube under an argon atmosphere. Decay profile measurements were carried out using the single photon timing technique[15] as described previously.[5,10,13,14] Phenanthrene decay profiles were monitored at 366 nm, with λ_{ex} = 300 nm. Decays were fitted to the expression

$$I(t') = A_1\left[\exp\left(-\frac{t'}{\tau_D} - P\left(\frac{t'}{\tau_D}\right)^{\beta}\right)\right] + A_2\exp\left(-\frac{t'}{\tau_D}\right) \quad (1)$$

with $\beta = 0.5$, and integrated as described in ref 19. Since here we are only interested in the integrated area under $I(t')$, i.e. the total fluorescence intensity, we do not here ascribe meaning to the individual parameters obtained from each decay curve.

Results and Discussion

Latex Characterization. MA0 contains only sulfate groups at the surface. The carboxylated latex samples, MA2, MA4, and MA6, were prepared using the MA0 samples as seeds, and the final stage polymer for these samples contains 2.0, 4.0, and 9.2 mol % methacrylic acid. The mean volume for MA0 is 1.13×10^6 nm³/particle, whereas for MA6 it is 1.75×10^6 nm³/particle. Thus in this sample the carboxylated copolymer represents approximately 35 vol % of the polymer in the particle.

The characteristics of the latex are given in Table 1. One sees that in the MA0 samples about one-third of the sulfate groups are titratable, implying that they lie either at the surface or just beneath the surface so that they become neutralized upon exposure to excess base. The rest of the sulfate groups remain buried in the interior of the particle. In the MA2, MA4, and MA6 samples, only about 10% of the sulfate groups are found in the surface region of the latex. In each of these samples, there is, however, a significant surface concentration of carboxylic acid groups. About 43% of the −COOH groups are to be found in the surface region of MA6. From a slightly different perspective, if the area

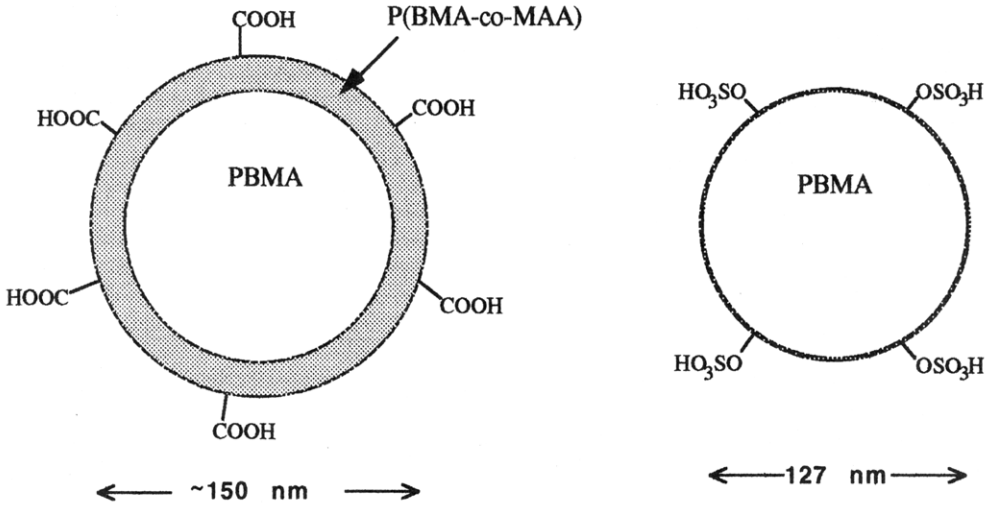

	mol% MAA	% titratable acid groups
MA2	2.0	56
MA4	4.0	60
MA6	9.2	44

Figure 1. Drawing depicting the size and composition of the latex samples MA0 and MA2–MA6. The acid groups which are not titratable in the aqueous dispersions are buried in the particle interior.

occupied by a COOH group is 25 Å^2, then half the total surface area of the MA6 particle is occupied by carboxylic acid functionality.

Data and Data Analysis. Fluorescence decay curves of some of the samples described in this have been published previously.[13,14] These decays are representative of all the samples examined here. As the polymers interdiffuse, more energy transfer takes place, leading to a more rapid decay of the fluorescence intensity. Each fluorescence decay curve represents a snapshot of the system following diffusion for a period of time t at an annealing temperature T_{an}. In light of the complexity of the samples, a detailed discussion of data analysis strategies is in order.

Theoretical Considerations. The detailed shape of the decay profile represents an integration over the distance distribution of donor–acceptor pairs. According to the theory of energy transfer in restricted geometries, the most rigorous approach to analyzing the decay profiles involves a double integration: for each locus of the donor, one integrates over the local acceptor distribution and then sums these integrals over the distribution of the donors.[16,17] An approximation to this difficult task, which works well when the spatial profile of donors and acceptors is not too steep, is to divide the interfacial space into a series of slices (for diffusion across a plane) or concentric spherical shells (for a spherical diffusion geometry), to assume that the acceptor concentration within each slide is uniform, and to sum over the donor concentration profile. This is the approach suggested recently by Dhinojwala and Torkelson[18] and also by Liu and Winnik.[19] These approaches require knowledge of the donor $C_D(r,t)$ and acceptor $C_A(r,t)$ concentration profiles, where r refers to the distance of D or A from the initial boundary between the donor- and acceptor-labeled polymers.

Since the area under each normalized fluorescence decay profile is equal to the total fluorescence intensity from the sample,[20] which in turn is proportional to the quantum efficiency of fluorescence ϕ_f, one could calculate quantum efficiencies of energy transfer ϕ_{ET} from changes in the area under the decay profiles. Alternatively, one could attempt to measure ϕ_{ET} by steady state fluorescence measurements. Appropriate equations and corresponding simulations for this approach were described recently by Dhinojwala and Torkelson.[18]

With an appropriate diffusion model, such as one derived from Fick's laws, $C_D(r,t)$ and $C_A(r,t)$ can be evaluated and introduced into the analysis of the fluorescence decay profile[17,19] (or the energy transfer efficiency[18]), using D_{cm} as the fitting parameter. This type of approach is particularly important when one is studying polymers of narrow molar mass distribution (i.e. characterized by a narrow distribution of diffusion coefficients) to obtain absolute D_{cm} values to be used for testing theory. For example, in spherical geometry, diffusion which satisfies Fick's laws is described by the equation[21]

$$\frac{\partial C(r,t)}{\partial t} = \frac{1}{r^2}\frac{\partial}{\partial r}\left(Dr^2\frac{\partial C(r,t)}{\partial r}\right) \tag{2}$$

so that at time t

$$C(r,t) = \frac{C_0}{2}\left\{\mathrm{erf}\left(\frac{R+r}{2\sqrt{Dt}}\right) + \mathrm{erf}\left(\frac{R-r}{2\sqrt{Dt}}\right)\right\} - \frac{C_0}{r}\sqrt{\frac{Dt}{\pi}} \times \left\{\exp\left(\frac{(R-r)^2}{4Dt}\right) - \exp\left(-\frac{(R+r)^2}{4Dt}\right)\right\} \tag{3}$$

In these expressions, the diffusion coefficient D refers either to D_{cm} or to D_{eff} as defined below.

Liu and Winnik[19] have used simulations to show that polymer samples with a significant polydispersity in D_{cm} values can still be analyzed in this way. What one obtains are good fits to individual fluorescence decay profiles, but the fitting parameter, now an effective diffusion coefficient D_{eff}, decreases with the increasing extent of interdiffusion. This result indicates that, within the context of the simulations, the fastest diffusing species contribute to the mixing process at early times, and that at later times, the species of smaller and smaller D_{cm} values contribute to the increase in energy transfer measured in the experiment. When the distribution of diffusing species is too broad, this type of analysis breaks down. One can introduce a *distribution of D values* into the fluorescence decay profile analysis. In spite of the success of our simulations, we still have some doubts about the meaningfulness of the distributions one can obtain from experimental data.

Different strategies are necessary when the distribution of diffusing species is large. One approach which we have employed in the past is to try to estimate the extent of mixing due to diffusion from comparison of the fluorescence decay curves. In terms of Fick's laws, the fraction of mass diffusing across the initial interface after time t is given by $f_s(t) = M_t/M_\infty$, where $M_\infty = (4/3)\pi R^3 C_0$, and

$$M_t = M_\infty - \int_0^R C(r,t)(4\pi r^2)\, dr \qquad (4)$$

If $f_s(t)$ could be determined experimentally, one could then integrate eq 4 numerically to find the best value of D_{eff}.

Another measure of the extent of mixing is expressed in terms of the fractional growth in energy transfer efficiency[10a,17]

$$f_m(t) = \frac{\phi_f(0) - \phi_f(t)}{\phi_f(0) - \phi_f(\infty)} = \frac{\text{area}(0) - \text{area}(t)}{\text{area}(0) - \text{area}(\infty)} \qquad (5)$$

In many of our previous publications,[10,13,14] we simply equated f_m to f_s and calculated diffusion coefficients via eqs 2–5. From a rigorous point of view, this approach is not justified theoretically, because the calculation of f_m neglects the concentration profile of diffusing species across the interface. Our analysis has been criticized rather forcefully, not only by Dhinojwala and Torkelson[18] but also by our co-worker Liu.[19] We treated this approach as a good approximation for two reasons: First, over much of the mixing process, $f_m(t)$ was found to be proportional to $t^{1/2}$, as expected for Fickian diffusion. Second, attempts to duplicate a very similar experiment which employed neutron scattering to determine interdiffusion gave remarkably similar values of D_{eff}.[22] Now, thanks to the theoretical analysis and simulations of Dhinojwala and Torkelson,[18] we have a deeper appreciation of the strengths and weaknesses of this approach.

Dhinojwala and Torkelson[18] examined the energy transfer experiment in lamellar geometry for polymers characterized by a unique diffusion coefficient. They find that the parameter $f_m(t)$ is proportional to $(D_{cm}t)^{1/2}$ during the early stages of the diffusion process and have evaluated the proportionality constant. Since $f_s(t)$ is also proportional to $(D_{cm}t)^{1/2}$ during these early stages, there is a significant range of the experiment where f_m is proportional to f_s. A key feature of their analysis is that the proportionality constant depends upon the acceptor concentration $C_{A,0}$ in the acceptor-labeled phase. Thus

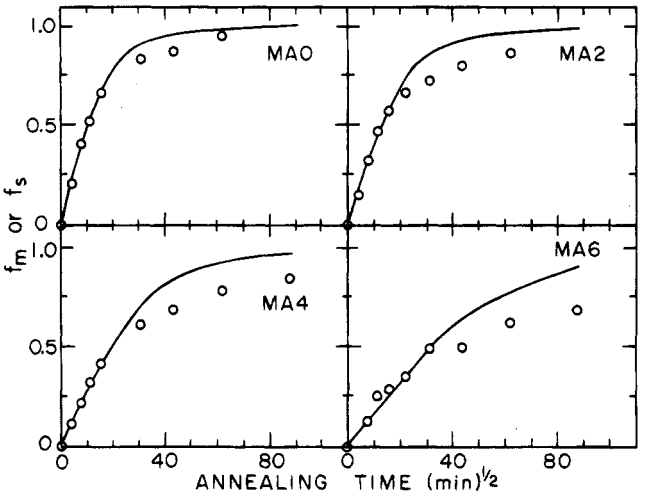

Figure 2. Plots of f_m values (open circles) calculated from the fluorescence decay data with eq 5 vs the square root of the sample annealing time at 90 °C for MA0–MA6 in the protonated form. The solid lines represent values of f_s calculated from a Fickian diffusion model in spherical geometry with a diffusion coefficient value selected to provide the best match between f_s and f_m at the early stages of diffusion. To calculate f_s, the following D values were employed: MA0, 6.5×10^{-16} cm^2 s^{-1}; MA2, 6.0×10^{-16} cm^2 s^{-1}; MA4, 62.7×10^{-16} cm^2 s^{-1}; MA6, 0.90×10^{-16} cm^2 s^{-1}. Reproduced from ref 13 with permission. Copyright 1994 Butterworth.

there is a narrow range of extent of labeling at which $f_m(t)$ and $f_s(t)$ are close in magnitude. Given the extent of labeling in our current samples, and on the basis of our own simulations, the calculated D_{eff} values differ from the "true" values by a factor of as much as 2–5. According to the simulations, the deviations become much more severe as $f_s(t) \to 1$. Errors of 10–100-fold or larger are possible.[23] Since, however, the experiment is carried out typically only to $f_m(t) = 0.8$ or 0.9, and $f_m(t)$ increases somewhat faster than $f_s(t)$, these large errors do not occur here.

One might ask, why calculate D values at all for such complicated systems? In our view, one needs a way of comparing different experiments. Typical variables of scientific and technological interest are the changes in diffusion rates which occur as temperature is varied, as plasticizers are added to the system, or as the chemical composition of the system is varied. As long as the extent of labeling (i.e. $C_{A,0}$) remains constant, and *different samples are compared at identical extents of mixing*, D values from different systems can be compared. Theories that describe changes in D_{cm} values as external parameters are varied, such as the Williams, Landol, Ferry [WLF][24] description of temperature effects or the Fujita–Doolitle[25] description of plasticizer effects, appear to apply equally well to D_{eff} values calculated in this way.[22,26]

Experimental Data. Representative data for films prepared from ion-exchanged samples of MA0–MA6 are shown in Figure 2. In these films the acid groups are present in their protonated form. The solid lines drawn in Figure 2 are plots of f_s vs diffusion time, in which the D_{cm} value was chosen so that the f_m data and f_s line coincide at early diffusion times. Our experiment differs from that described by the simulations and the theory in that we employ a 1:1 mixture of D- and A-labeled microspheres. Nevertheless, we note that especially for MA0 and MA2 in Figure 2 that f_m is proportional to $t^{1/2}$ over significant portions of the interdiffusion process. To simplify the analysis and permit comparison of the

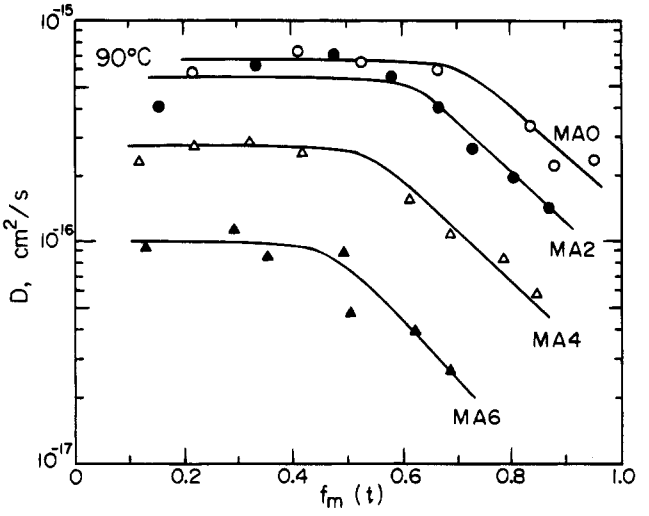

Figure 3. D_{app} values calculated from the f_m data in Figure 2, plotted as a function of the extent of mixing.

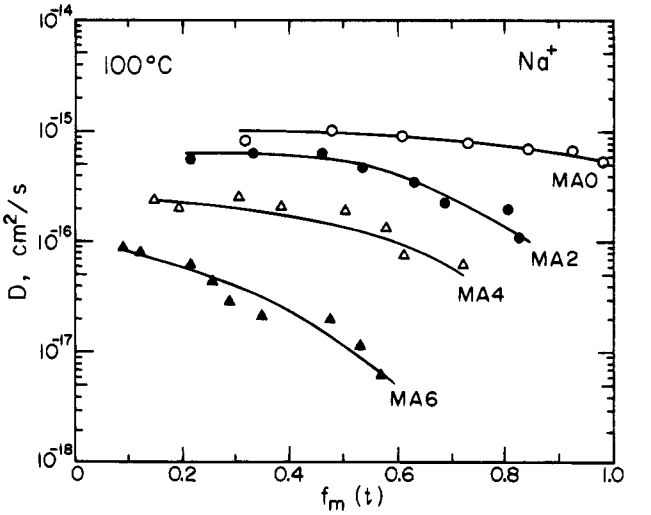

Figure 4. D_{app} values obtained for latex film samples prepared from dispersions in which 1.0 equiv of NaOH was added, based upon the moles of titratable acid groups in the sample: (○) MA0, (●) MA2, (△) MA4, (▲) MA6.

different samples as described above, we will assume that $f_m = f_s$, recognizing that they likely differ by a constant factor over much of the diffusion process.

To emphasize the difference between the actual D_{eff} values characterizing diffusion in these systems and those calculated by assuming that $f_m = f_s$, we refer to our experimental values as apparent diffusion coefficients D_{app}. Thus to calculate mean apparent diffusion coefficients for each experiment at each annealing time, we seek the value of D which, in terms of a spherical Fickian diffusion model, gives a value of f_s best approximating the f_m determined in the experiment.

Surface Functionality and Interdiffusion Rates. Diffusion coefficients calculated as described above for the data in Figure 2 are plotted in Figure 3. The essential feature of these data, for films annealed at 90 °C, is that for the sample MA0, which contains only a small number of $-OSO_3H$ groups, the interdiffusion process can be described by a single D_{app} value over a large span of f_m. In MA2, MA4, and MA6, there is a progressive decrease in the early time value of D_{app}, but a more significant feature of the data is the earlier onset of the decrease in D_{app} with the increase in f_m. We interpret this behavior to indicate that as the distribution of diffusing species in the sample broadens, one is less able to describe the diffusion process in terms of a single average D_{app} value. To pursue this analysis further, we suggest that the retardation of D_{app} at early times is indicative of the need for the fastest diffusing species in the system to diffuse through a region of higher local friction, and the pronounced decrease in D_{app} indicates the onset of mixing of chains of intrinsically lower mobility, i.e. those copolymers containing the carboxylic acid group functionality.

A second example of this type of retardation can be seen in Figure 4 where we compare films prepared from the same four latex samples after the addition of 1 equiv of NaOH per titratable acid group in the dispersion. Diffusion is slower here, and these samples are annealed at 100 °C. The same general features are seen here as in Figure 3, except that there is no sharp onset of curvature. D_{app} values decrease with the increase in the concentration of $-COO-Na^+$ groups and also decrease with the increasing extent of mixing. We return to this point when we examine ionomer effects in more detail below.

Temperature Effects. Early work from our laboratory on latex samples similar in structure to MA0

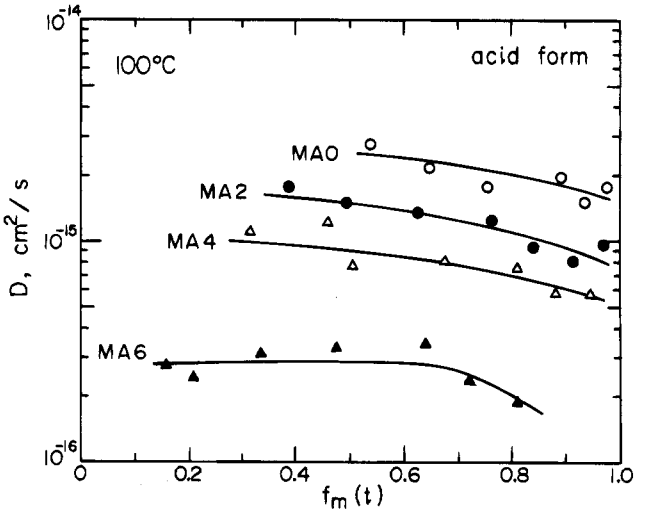

Figure 5. D_{app} values obtained for latex films prepared from ion-exchanged dispersions and annealed for various times at 100 °C: (○) MA0, (●) MA2, (△) MA4, (▲) MA6.

examined the temperature dependence of the polymer interdiffusion rate. Two samples of very different molecular weights (and thus very different D_{app} values) were characterized by essentially identical apparent activation energies E_a^{app} when compared at similar f_m values, and plots of D_{app} vs f_m at different temperatures could be reduced to a single master curve using WLF parameters obtained by Ferry[27] from creep compliance measurements on PBMA many years earlier.

We observe quite different behavior for the samples examined here. In Figure 5 we show D_{app} values for latex films annealed at 100 °C for the same four samples shown in Figure 3. For the samples MA4, MA2, and MA0, it is progressively more difficult to obtain data at early annealing times because the diffusion rate is now much faster than that at 90 °C. The same trend in decreasing D_{app} values with increasing acid group concentration is observed, but the sharp break seen in the curves in Figure 3 is not apparent here except perhaps in the MA6 sample.

To emphasize the influence of annealing temperature on the shape of the D_{app} vs f_m plot, we compare in Figure 6 D_{app} values calculated from experiments carried out

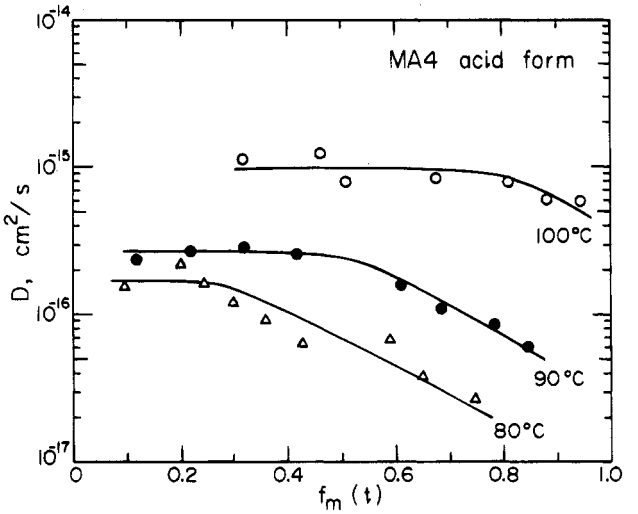

Figure 6. D_{app} values obtained for latex films prepared from an ion-exchanged sample of MA4 and annealed at different temperatures: upper curve, 100 °C; middle curve, 90 °C; lower curve, 80 °C.

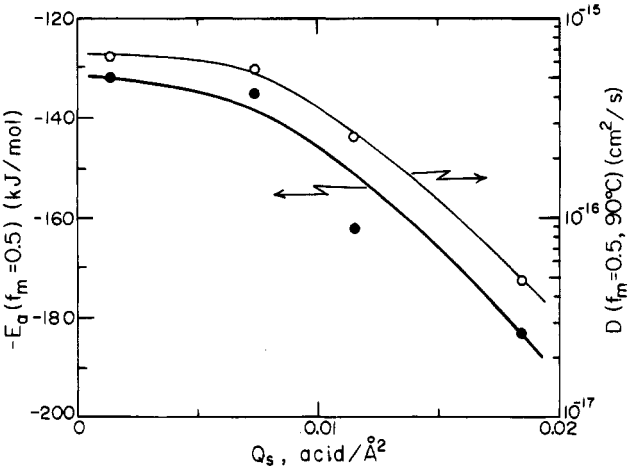

Figure 7. Plot of apparent activation energies E_a^{app} (closed circles, left ordinate) for samples MA0–MA6 against the area per surface acid group determined from titration of the latex. E_a^{app} values were obtained from Arrhenius plots of log D_{app} vs T^{-1} for D_{app} values obtained at f_m = 0.5. The right-hand ordinate (open circles) indicates the magnitude af D_{app} at f_m = 0.5 in each sample.

for MA4 at three different temperatures. Raising the temperature has the effect of not only increasing the early time D_{app} values but also narrowing the distribution of diffusion rates in the system. If one compares the magnitude of the temperature-induced changes in the system at early, intermediate, and late times, one suspects that the apparent activation energies calculated from the data would increase as the extent of interdiffusion proceeds. Data from MA0, MA2, MA4, and MA6 give linear Arrhenius plots for the three temperatures when compared at f_m = 0.3, 0.5, and 0.7, with E_a^{app} at similar f_m increasing with an increasing number of acid groups in the sample. These E_a^{app} values are compared in Figure 7 for data obtained at f_m = 0.5, plotted as a function of the number of titratable acid groups per Å^2 of surface area in each latex. The filled circles refer to the magnitude of E_a^{app}, which increases from 130 kJ/mol for MA0 to 185 kJ/mol for MA6. The open circles (right-hand ordinate) plot the values of D_{app} for each sample at 90 °C.

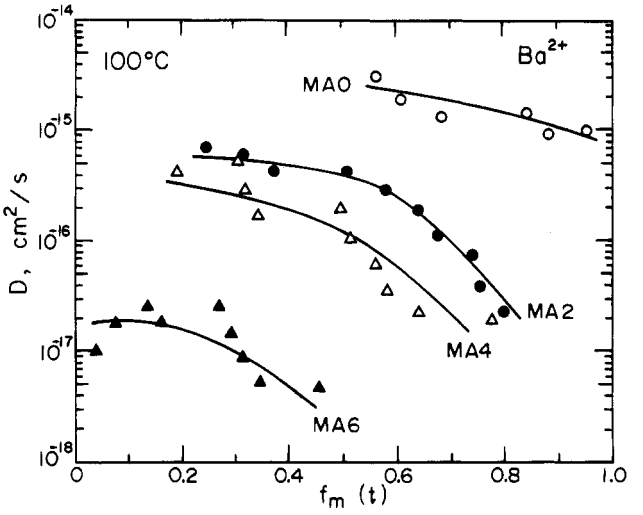

Figure 8. D_{app} values obtained for latex film samples prepared from dispersions in which 1.0 equiv of $Ba(OH)_2$ was added, based upon the moles of titratable acid groups in the sample: (○) MA0, (●) MA2, (△) MA4, (▲) MA6.

Ionomer Effects. In Figure 4, we observe that neutralization of the carboxyl groups in the latex dispersion with NaOH yields films with retarded interdiffusion rates. In Figure 8, we present similar data for the same four samples here neutralized with 1 equiv of $Ba(OH)_2$ per titratable acid group. The retardation in interdiffusion rate is now much more severe, decreasing by more than 2 orders of magnitude between MA0 and MA6. There is once again a sharp downward break in the D_{app} vs f_m plot for the MA2 and MA4 films. Diffusion is so slow for the barium-neutralized MA6 sample that we have difficulty obtaining D_{app} values with good precision.

In the previous sets of samples, we added 1 equiv of base to each dispersion calculated on the numbers of moles of titratable acid groups in each sample. We also wished to examine the influence of the amount of base added on the interdiffusion rate. Since approximately half the −COOH groups in each latex are buried in the latex interior, it is also possible that adding excess base compared to surface acid groups might influence polymer diffusion. In Figure 9 we compare five different experiments involving MA6. Here the dispersion of MA6 was treated with varying amounts of sodium hydroxide prior to film formation. The top curve repeats the data for the ion-exchanged sample (−COOH form). The amount of NaOH added corresponds to 0.25, 0.50, 0.75, 1.0, and 1.5 times the number of titratable −COOH groups in the sample.

Progressive neutralization of the acid groups leads to a significant decrease in the early time D_{app} values and an earlier onset of the decrease in their magnitude. There is some suggestion in the data that for the sample in which the amount of NaOH added exceeds the amount of acid groups near the surface of the latex, the initial D_{app} is determined only by the initially neutralized acid groups and the onset of interdiffusion leads to further neutralization of the remaining acid groups until all the NaOH is consumed. If these data are all compared at f_m = 0.5, we find a linear relationship (Figure 10) between the magnitude of log D_{app} and the number of neutralized acid groups.

Model for the Polar Group Effect. The increase in apparent activation energy with increasing acid group content in the polymer suggested to us that the glass transition temperature of the polar phase might be the

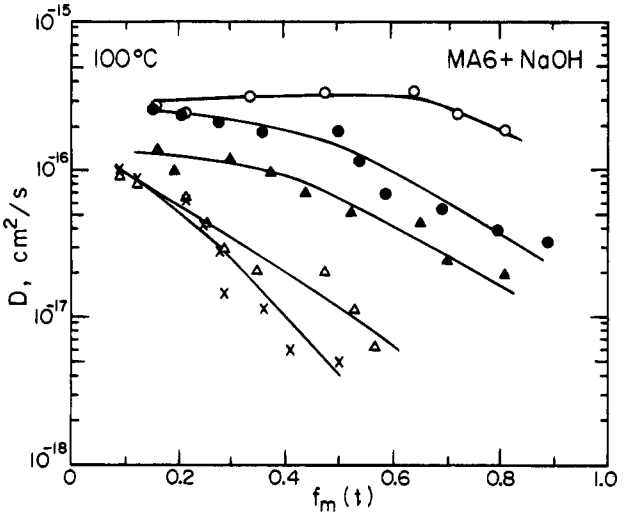

Figure 9. Plot of D_{app} vs f_m for films prepared from MA6 as a function of the amount of NaOH added to the dispersion prior to film formation. The amounts of base added correspond (top to bottom) to 0%, 25%, 50%, 100%, and 150% of the number of moles of titratable acid groups in the latex.

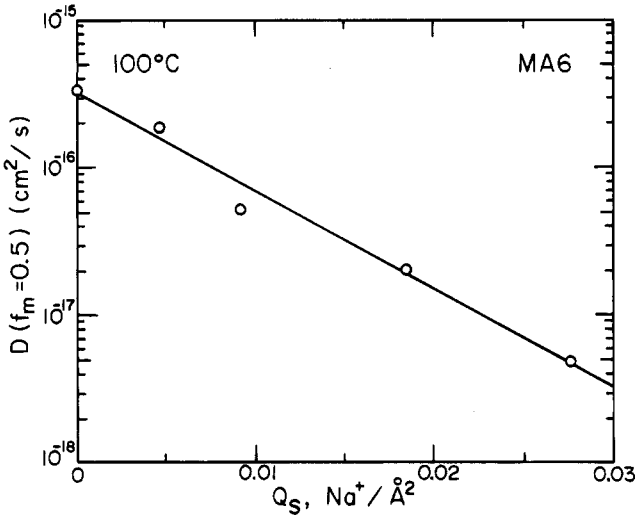

Figure 10. Plot of D_{app} values obtained at $f_m = 0.5$, using the data in Figure 9 for films prepared from MA6 as a function of the amount of NaOH added to the dispersion prior to film formation. The x-axis is in units of number of Na^+ ions per Å^2 of latex surface area. The amounts of base added correspond to 0%, 25%, 50%, 100%, and 150% of the number of moles of titratable acid groups in the latex.

most important parameter affecting the polymer interdiffusion rate. The simplest model incorporating these ideas is one in which we consider that the latex particles themselves have a core–shell structure, with a PBMA homopolymer core surrounded by a shell of the third-stage copolymer. Such particles would produce a film in which cells of the PBMA homopolymer would be separated from one another by a membrane composed of the copolymer, whose T_g would depend upon the acid group content, the extent of neutralization, and the ionic charge of the cation in this ionomer phase. We begin our analysis by trying to estimate the local T_g of this phase and then proceed by comparing the diffusion rates for different values of $(T - T_g)$, where T refers to the annealing temperature.

Estimating T_g. Values of T_g for copolymers can be estimated either from the Flory–Fox equation[28] or via an expression found empirically by Eisenberg[29] for ionomer samples. Eisenberg found that for a series of copolymers containing acid or ionic groups, T_g increased linearly with ionic group content according to the expression

$$T_g \propto c\frac{q}{a} \tag{6}$$

where c is the mole fraction of acid or ionic group in the copolymer, q is the ionic charge, and a is the characteristic distance representing the center-to-center separation of the cation and anion in the ion pair.[29] To proceed, we need values of the corresponding homopolymers, PBMA, poly(methacrylic acid), PMAA, its fully neutralized sodium salt, PMAA–Na^+, and the corresponding barium salt, PMAA–Ba^{2+}. We note that there is significant scatter in the literature values. No value for the barium salt of poly(methacrylic acid) is available in the literature, but a value for the corresponding magnesium salt is reported, and we use this value in our analysis. These T_g values are collected in Table 2, as are the values of $\partial T_g/\partial c$ calculated from eq 3. The values of $\partial T_g/\partial c$ calculated for PBMA–PMAA and for PBMA–PMAA–Na^+ are very similar to those obtained by Eisenberg[29] for acrylic acid–ethyl acrylate copolymers ($\partial T_g/\partial c$ = 1.3 °C/mol %) and for sodium acrylate–ethyl acrylate copolymers ($\partial T_g/\partial c$ = 2.9 °C/mol %) over the range of 4–12 mol % carboxylate.

Table 2. Glass Transition Temperatures and T_g Increments of the Copolymers

polymer	T_g	polymer	$\partial T_g/\partial c$ (°C/mol %)
PBMA	308[a]		
PMAA	458[a,b]	PBMA–PMAA	1.50
PMAA–Na^+	583[c]	PBMA–PMAA(Na^+)	2.75
PMAA–Mg^{2+}	763[a,c,d]	PBMA-PMAA(Mg^{2+})	4.55

[a] Brandrup, J.; Immergut, E. H. *Polymer Handbook*, 3rd ed.; Wiley-Interscience: New York, 1989. For PBMA, by DSC, we find 308 °C. [b] Razinskaya, I. N.; Kharitonova, B. P.; Shtarkman, B. P. *Vysokomol. Soedin. B* **1969**, *11*, 892. [c] Otocta, E. P.; Kwei, T. K. *Macromolecules* **1968**, *1*, 401. [d] No value for the barium salt could be found.

From these values, we calculate the T_g of the membrane phase from the composition of shell phase of the latex:

$$T_{g(\text{membrane})} = 308 + \partial T_g/\partial c_{\text{PMAA–H}}\, c_{\text{PMAA–H}} + \partial T_g/\partial c_{\text{PMMA–salt}}\, c_{\text{PMAA–salt}} \tag{7}$$

Here the term $c_{(\text{PMAA–H})}$ refers to the mol fraction of PMAA, and $c_{(\text{PMAA–salt})}$ to the corresponding salt, respectively. The values of $c_{(\text{PMAA–H})}$ and $c_{(\text{PMAA–salt})}$ used in these calculations and the values of T_g obtained are collected in Table 3.

The changes in T_g predicted in this way are relatively small. That makes these changes difficult to measure. For example, by DSC we can detect no difference in behavior between a film of MA0 and MA6. We also note that these films are all transparent and that films cast from a solvent such as THF also yield transparent films. This implies that at this low level of acid group incorporation, there is either a certain degree of miscibility between the homopolymer and copolymer phases, or the changes in index of refraction between the two phases are too small to scatter light significantly.

Relating D_{app} to $(T - T_g)$. We have two independent sets of data which can be used to evaluate relationships between D_{app} and $T - T_g$, where T_g refers to those values calculated for the membrane phase of the films. One set of experiments involves films prepared from the

Table 3. Composition and Calculated T_g Values for the Shell Phase of Latex Particles MA0–MA6

	[PMMA-H] (mol %)	[PMMA-X] (mol %)	T_g (Na^+) (K)	T_g (Ba^{2+}) (K)	T_g (–H)[a] (K)
One Equivalent of Base Per Titratable Acid Group					
MA0	0.0	0.0			308
MA2	0.40	1.6	313	316	311
MA4	0.84	3.16	318	324	314
MA6	4.69	4.50	327	336	322
MA6 Plus Varying Amounts of NaOH					
MA6–0.25[b]	8.06	1.13	323		
MA6–0.50	6.94	2.25	325		
MA6–1.50	2.44	6.75	330		

[a] T_g of the fully ion-exchanged latex with all carboxylic acid groups in the protonated form. [b] Amount of NaOH added to the sample as a fraction of acid groups titratable in aqueous solution.

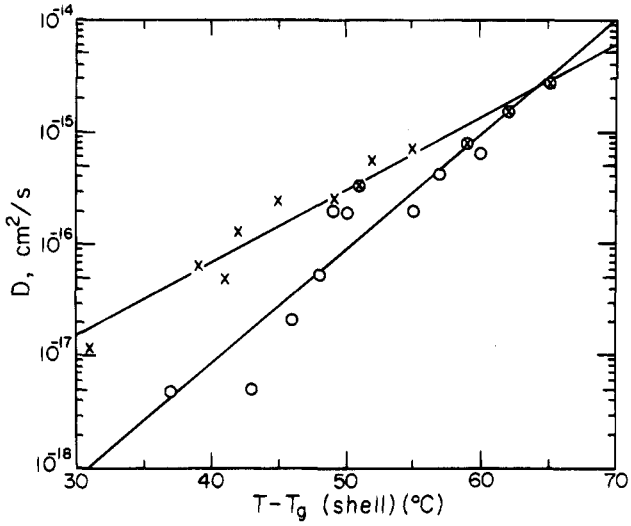

Figure 11. Plot of log D_{app} vs $(T - T_g)$ for D_{app} values obtained at $f_m = 0.5$ for all the experiments reported in this paper. The data points indicated by × refer to the latex with the acid groups in the protonated form, obtained at three different temperatures. The data points denoted by open circles refer to film samples of latex neutralized by barium hydroxide or sodium hydroxide and studied at 100 °C. The four points representing MA0–MA6 in the protonated form and obtained at 100 °C are used in the fit of both lines.

ion-exchanged latex, with the acid groups present in the protonated form. We have data for three carboxylated latex samples examined at three different temperatures. The second set of samples involves the same series of latex, partially neutralized with different quantities of sodium and barium hydroxide but examined at only one temperature. Here T remains constant, but T_g varies. On the basis of the idea that $\log(1/\eta)$ varies with $(T - T_g)$ for polymer melts,[24] we plot values of log D_{app} obtained at $f_m = 0.5$ vs $T - T_g$ for the films with the protonated carboxylate groups, and for the ionomer films in Figure 11. The data for the former set of samples in Figure 11 yield a reasonably straight line with a slope of 1.16 and an intercept of 1.7×10^{-19} cm^2 s^{-1}. The data for the ionomer films give the lower set of data in Figure 11. They fit less well to a straight line ($R^2 = 0.90$), but the best-fit line has a slope of 1.27 and an intercept of ca. 10^{-22} cm^2 s^{-1}.

We take the linear plots in Figure 11 as a strong indication of the role of the glass transition temperature of the membrane in determining interdiffusion rates in these latex films. The fact that the data do not fall onto a common line for the acids and the salts may indicate that for similar estimated $(T - T_g)$ values, ion pairs or ion clusters are somewhat more effective at retarding diffusion than are the protonated acid groups themselves. Or it may reflect limitations in the various assumptions we have made in calculating $(T - T_g)$.

The most important question, which we cannot answer unambiguously at this time, is which polymers are diffusing at the earliest stages of the mixing process. Many scientists in the coatings area believe that in such systems the membrane polymers mix and then phase separate, and only at that point can the core polymers interdiffuse. This is almost certainly the case for core–shell latex films in which the membrane is very thin and composed of a polar polymer such as poly(acrylic acid) poorly miscible with the core polymer. In such systems, it is likely that the membranes must fracture and coalesce into phase-separated droplets before interdiffusion of the remaining polymer can occur.[12]

Here we have a very different situation. There is no evidence that the core and shell polymers are immiscible. The energy transfer experiments indicate that the fastest diffusing polymers undergo mixing at the earliest stages of annealing. Experiments in which temperature is a variable indicate that the apparent activation energy increases with the extent of interdiffusion. This is seen not only in Figure 7 but also in Figures 5 and 6, where at elevated temperatures, the changes in D_{app} diminish, implying a narrowing of the distribution of D values in the system.

The polymers with the highest diffusivity are the lowest molecular weight components of the PBMA core homopolymer. Diffusivity decreases both with increasing molecular weight and with carboxyl content of the copolymer chains. These observations lead to a different suggestion, namely that at the early stages of annealing, it is the core homopolymer which is diffusing through the membrane phase to mix with the core homopolymer in adjacent cells. Some of this many occur because the latex morphology may not be sharply delineated between a core and a shell phase: phase mixing during latex synthesis in which some core polymer becomes part of the shell would contribute to this effect.

A drawing depicting the two possible mixing processes is presented in Figure 12. While no firm conclusion can be drawn at this time, one should in fact be able to examine the situation more deeply by preparing polymers analogous to MA6 in which only the homopolymer or copolymer stage is labeled. In this way one ought be able to assess which phases are able to mix, and the timing of the interdiffusion of the various components in the system.

Summary

We report measurements of the kinetics of polymer diffusion in latex films prepared from pairs of poly(butyl methacrylate) [PBMA] latex particles. One set contains only a small amount of sulfate groups; the others contain significant amounts of carboxylic acid groups at the surface. Neutralization of these acid groups with sodium and barium hydroxide retards the interdiffusion rate but does not suppress it. Acid group neutralization in the latex converts an acid-rich phase at the interparticle boundary in the film into an ionomer phase. Ba^{2+} salts are more effective than Na^+ at slowing down the polymer diffusion rate, and their influence increases in proportion to the amount of polar groups present. We estimate the T_g values of the ionomer phase in each film, and show that there is a linear relationship between the log of the mean apparent diffusion coefficient of the polymer determined from the DET experiment and $T - T_g$, where T is the annealing temperature of the film.

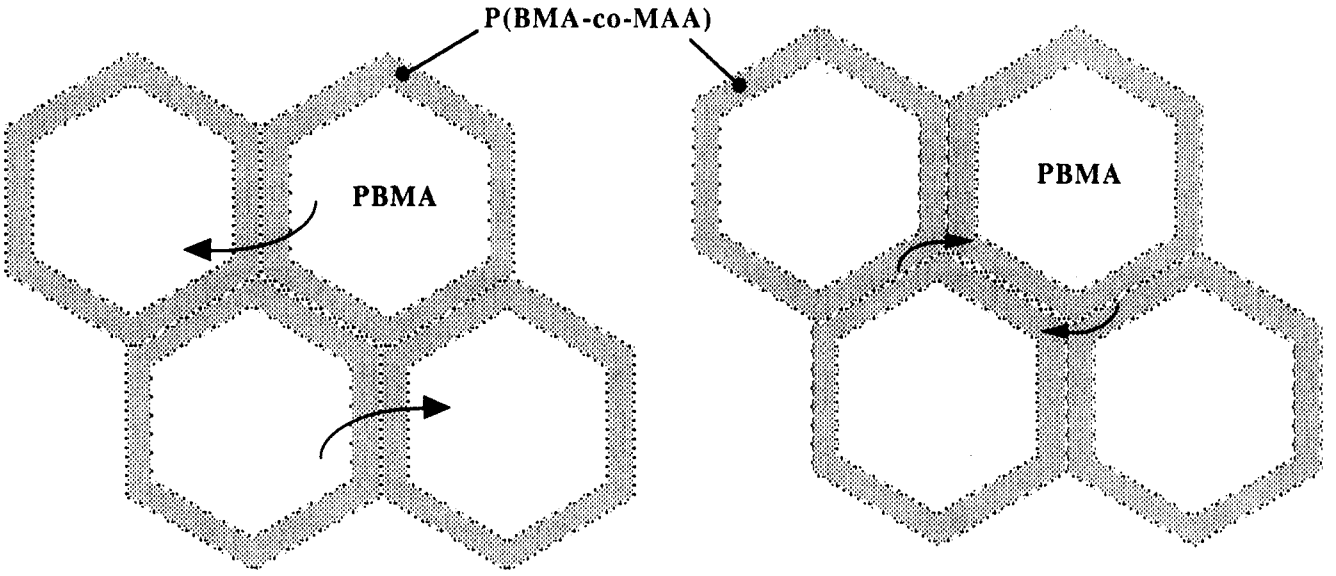

POLYMER DIFFUSION IN FILMS OF MA6

Figure 12. Drawing suggesting two possibilities for the species contributing to the mixing process at early times. On the left, early stage diffusion involves mixing of the membrane polymers. Because of their functional groups, one might expect them to be the least mobile components in the system. On the right, early stage diffusion involves mixing of the core polymers which are obliged to diffuse through the membrane composed of the more polar polymer.

Acknowledgment. The authors thank the Glidden Co., ICI, ICI Canada, and NSERC Canada for their support of this research and Dr. S. Kawaguchi for his helpful comments.

References and Notes

(1) Paper No. 4 in a series on the effect of polar material on polymer interdiffusion in latex films. For papers No. 1–3, see refs 13 and 14.
(2) Permanent address: Department of Chemistry, Faculty of Engineering, Hokkaido University, Sapporo 060, Japan.
(3) Paton, T. C. *Paint Flow and Pigment Technology*; Wiley: New York, 1979.
(4) Voyutskii, S. S. *Autohesion and Adhesion of High Polymers*; Wiley-Interscience: New York, 1963.
(5) (a) Wang, Y.; Winnik, M. A.; Haley, F. *J. Coat. Technol.* **1992**, *64* (811), 51. (b) Wang, Y.; Winnik, M. A. *J. Phys. Chem.* **1993**, *97*, 2507.
(6) Hahn, K.; Ley, G.; Schuller, H.; Oberthur, R. *Colloid Polym. Sci.* **1986**, *264*, 1092.
(7) de Gennes, P. G. *C. R. Acad. Sci. Ser. B* **1980**, *291*, 219.
(8) (a) Wool, R. P.; O'Conner, K. M. *J. Appl. Phys.* **1981**, *52*, 5194, 5953. (b) Kim, Y. H.; Wool, R. P. *Macromolecules* **1983**, *16*, 1115. (c) Wool, R. P.; Yuan, B.-L.; McGarel, O. J. *Polym. Eng. Sci.* **1989**, *29*, 1340.
(9) (a) Prager, S.; Tirrell, M. *J. Chem. Phys.* **1981**, *75*, 5194. (b) Prager, S.; Adolf, D.; Tirrell, M. *J. Chem. Phys.* **1983**, *78*, 7015. (c) Prager, S.; Adolf, D.; Tirrell, M. *J. Chem. Phys.* **1986**, *84*, 5152.
(10) (a) Wang, Y.; Winnik, M. A. *Macromolecules* **1993**, *26*, 3147. (b) Li, L.; Wang, Y.; Winnik, M. A.; Yan, H.; North, T. H. *Macromolecules*, in preparation.
(11) (a) Yoo, J. N.; Sperling, L. H.; Glinka, C. J.; Klein, A. *Macromolecules* **1990**, *23*, 3962. (b) Yoo, J. N.; Sperling, L. H.; Glinka, C. J.; Klein, A. *Macromolecules* **1991**, *24*, 2868. (c) Mohammadi, N.; Yoo, J. N.; Klein, A.; Sperling, L. H. *J. Polym. Sci., Part B: Polym. Phys.* **1992**, *30*, 1311.
(12) (a) Joanicot, M.; Wong, K.; Richard, J.; Maquet, J.; Cabane, B. *Macromolecules* **1993**, *26*, 3168. (b) Joanicot, M. Personal communication. (c) Chevalier, Y.; Pichot, C.; Graillat, C.; Joanicot, M.; Wong, K.; Lindner, P.; Cabane, B. *Colloid Polym. Sci.* **1992**, *270*, 806.
(13) Kim, H.-B.; Wang, Y.; Winnik, M. A. *Polymer* **1994**, *35*, 1779.
(14) (a) Kim, H.-B.; Winnik, M. A. *Macromolecules* **1994**, 427, 1007. (b) Winnik, M. A.; Kim, H.-B.; Kawaguchi, S. In *Progress in Pacific Polymer Science 3*; Ghiggino, K. P., ed.; Springer-Verlag: Berlin, 1994; p 247.
(15) O'Connor, D. V.; Phillips, D. *Time-Correlated Single Photon Counting*; Academic Press: New York, 1984.
(16) (a) Klafter, J.; Blumen, A. *J. Chem. Phys.* **1984**, *80*, 875. (b) Blumen, A.; Klafter, J.; Zumhofen, G. *J. Chem. Phys.* **1986**, *84*, 1397.
(17) Yekta, A.; Duhamel, J.; Winnik, M. A. *Chem. Phys. Lett.* in press.
(18) Dhinojwala, A.; Torkelson, J. M. *Macromolecules* **1994**, *27*, 4817.
(19) (a) Liu, Y. S.; Li, L.; Ni, S.; Winnik, M. A. *Chem. Phys.* **1993**, *177*, 579. (b) Liu, Y. S.; Feng, J.; Winnik, M. A. *J. Chem. Phys.* **1994**, *101*, 9096. (c) Winnik, M. A.; Liu, Y. S. *Makromol. Chem. Macromol. Symp.*, in press.
(20) Birks, J. B. *Photophysics of Aromatic Molecules*; Wiley: New York, 1970.
(21) Crank, J. *The Mathematics of Diffusion*; Clarendon Press: Oxford, 1975.
(22) Wang, Y.; Winnik, M. A. *J. Chem. Phys.* **1991**, *95*, 2143.
(23) Farinha, J. P. S.; Martinho, J. M. G.; Yekta, A.; Winnik, M. A. *J. Phys. Chem.* in press.
(24) Ferry, J. *Viscoelastic Properties of Polymers*, 3rd ed.; Wiley: New York, 1980; p 289.
(25) Fujita, H. *Fortschr. Hochpolym.-Forsch.* **1961**, *3*, 1.
(26) Juhué, D.; Wang, Y.; Winnik, M. A. *Makromol. Chem. Rapid Commun.* **1993**, *14*, 345.
(27) Child, W. C., Jr.; Ferry, J. D. *J. Colloid Sci.* **1957**, *12*, 327.
(28) Sperling, L. H. *Introduction to Physical Polymer Science*; Wiley-Interscience: New York, 1986; p 277.
(29) (a) Eisenberg, A. *Macromolecules* **1971**, *4*, 125. (b) Matsuura, H.; Eisenberg, A. *J. Polym. Sci., Polym. Phys. Ed.* **1976**, *14*, 1201.

MA945052L